12th IEA Heat Pump Conference 2017

Metal Wire Structures as Heat Transfer Surface Area Enlargement – Design Study and Potential Analysis for Air-to-Water Heat Pumps

Hannes Fugmann[a], Thore Oltersdorf [a], Lena Schnabel [a]*

[a] Fraunhofer ISE, Fraunhofer Institute for Solar Energy Systems, Heidenhofstr. 2, 79110 Freiburg, Germany

Abstract

It is common practice in air-to-water heat pumps to use fin-and-tube heat exchangers as evaporators. The typically used heat exchanger concept is based on round tubes which are connected by non-adhesive joints. The surface area enlargement for tubes in the range of 15mm down to 5mm is about 3.5-20. Other concepts like the so-called microchannel heat exchanger uses typically adhesive joints reaches similar surface area enlargements for stationary equipment.
In order to increase the surface area further on, without using more material, wire structures can be used as fins instead of metal sheets. In addition fluid flow along wire-based structures experiences a very high heat transfer coefficient due to the repeating interruptions and small dimensions.
New textile developments enable the fabrication of adapted structures with non-regular grid sizes purpose-built for gas to liquid and gas to gas/liquid heat exchanger application. At Fraunhofer ISE a variety of textile structure heat exchanger samples has been manufactured and evaluated.
In this paper a simulation study for different geometries of a flat tube wire structure heat exchanger will be performed and the integration into air-driven evaporators of residential heat pumps will be discussed. The results will indicate the potential of wire structures with respect to performance enhancement, material usage and size.

Selection and/or peer-review under responsibility of the organizers of the 12th IEA Heat Pump Conference 2017.

Keywords: Air-to-water heat pump; wire structure; heat transfer; fluid dynamics

Nomenclature

a	non-dimensional fin pitch $a = \mathrm{l}_{\mathrm{lateral}}/d_{\mathrm{wire}}$
A	area (m²)
b	non-dimensional wire distance in air flow direction $b = \mathrm{l}_{\mathrm{longitudinal}}/d_{\mathrm{wire}}$
c_p	specific heat capacity (J/kg K)
d_{wire}	diameter or wire (m)
f	friction factor
h	convection heat transfer coefficient (W/m² K)
H	height
k	thermal conductivity (W/m K)

* Corresponding author. Tel.: +49-761-4588-5412; fax: +49-761-4588-90 00.
E-mail address: lena.schnabel@ise.fraunhofer.de.

L or l	length (m)
m	mass (kg)
Nu	Nusselt number
p	pressure (Pa)
Pr	Prandtl number
$\dot{Q}$	heat transfer rate (W)
Re	Reynolds number
T	temperature (K)
U	overall heat transfer coefficient (W/m² K)
V	volume (m³)
Greek symbols	
β	heat transfer surface area density (m²/m³)
δ	thickness of walls or fins (m)
η_0	extended surface efficiency
ν	kinematic viscosity (m²/s)
ρ	density (kg/m³)
ϕ	porosity
Subscripts	
air	air side
HTS	heat transfer surface
HX	heat exchanger
st	domain between tubes for heat transfer enhancement structure
w	water side
fin	fins/wires for heat transfer enhancement
lateral / longitudinal	perpendicular to / in direction of major flow direction

1. Introduction

Metal textile structures are widely investigated in regenerative heat exchanger [1], solar energy collectors [2], electronic cooling [3] and other heat transfer applications. The main reason for their usage is a large value of surface area density. Essential differences in application are first that the wire structures are used as thermal storage, second that the wire structures transfer heat by conduction. We concentrate in this article on oriented wire structures designed for conductive heat transport along the wire and high convective heat transport on the wire surface area. Therefore these wire structure compete with standard fins, such as wavy fins, offset strip fins or multi-louvered fins [4] based on metal sheets. Louvered fins were investigated for conventional fin-and-tube heat exchangers as evaporators in [5–8].

A variety of design ideas for wire structure heat exchangers on flat tubes are shown in literature. Liu, Xu et al. and other authors [9–11] contact metallic woven wire mesh structures to a flat primary surface, separating the fluid from the heat source or sink. In [12] screen-fin structures are used instead of woven wire mesh structures.

Tian et al. [13] and Li et al. [14] present wire structure heat exchangers formed of woven fabrics in sandwich form. The textile cellular metal core sandwich panels in [13] are realized with wire diameters of 0.8 mm and higher. They show volume specific heat transfer surface areas of less than 1500 m²/m³. Individual mesh layers are stacked peak-to-peak, either by a brazing alloy or a transient liquid phase alloy, creating the cellular metal core.

Sahiti et al. [15–17] and Bhunte et al. [18] perform thermal hydraulic simulation of pin fin structures. The pins have diameter of more than 0.5 mm. They are arranged in parallel between a bottom and top plate. Volume specific performance of pin fin structures is rated higher than for corrugated fins. Manufacturing processes are not described. Usual application of pin fins is given in cooling of electronic devices. The pins are generally cut to length and thereafter contacted to bottom and top plates by e.g. laser welding [19]. This structure is denominated

as discontinuous parallel wire structure, as the pin fins are interrupted. The pin fin structure differs in manufacturing from woven or knitted structures; however the final geometry in a flat tube heat exchanger can be similar. A commercially available technology of continuous parallel wire structure is provided by the Dutch company Vision4Energy [20]. Two gases flow primarily in cross-flow arrangement, separated by a dividing wall.

Much of the literature focuses either on wire diameter in the range of 0.5 mm in pin fin design or on wire meshes with non-oriented wires. We have focused in this study on compact heat exchangers with surface enhancement based on oriented wire structures with diameter in the range of 0.1mm. One fluid in the heat exchanger was air. This study shall illustrate if heat transfer surface area enhancement with textile structures can exceed hydraulic and/or thermal performance of louvered fins. The authors concentrate on flat tube heat exchangers. A design idea is shown in Fig. 1. The authors show different arrangements of wires for this design idea and evaluate performance based on CFD-simulation. They compare the results to a measurement of a commercially available pin fin heat exchanger and literature correlation for a louvered fin heat exchanger.

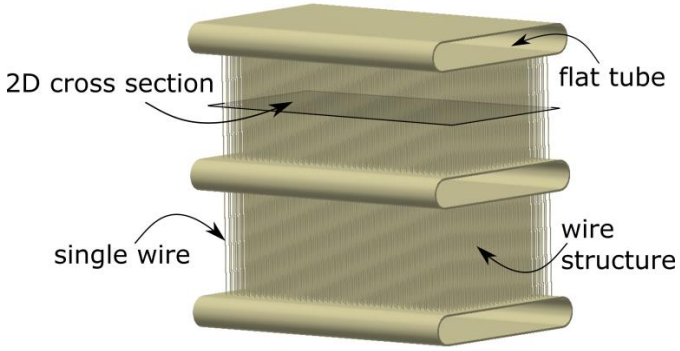

Fig. 1. Vertical oriented wire structures between flat tubes. Wire structure consists of a variety of single wires. 2D cross section through the structure for later simulation in black [21].

2. Design Idea and Experimental Setup

In the project EffiMet [22] different knitted fabrics have been manufactured at the textile manufacturer Visiotex [23]. All fabrics served as basis for heat transfer surface area enhancement. The target was to show feasibility of manufacturing wire structure heat exchanger based on irregular knitted fabrics. The fabrics were composed of very dense domains and very open domains. The very dense domains provided the basis for a fluid separating wall, in the open domains gas flowed around the structure. One fabric is presented in Fig. 2 (left side).

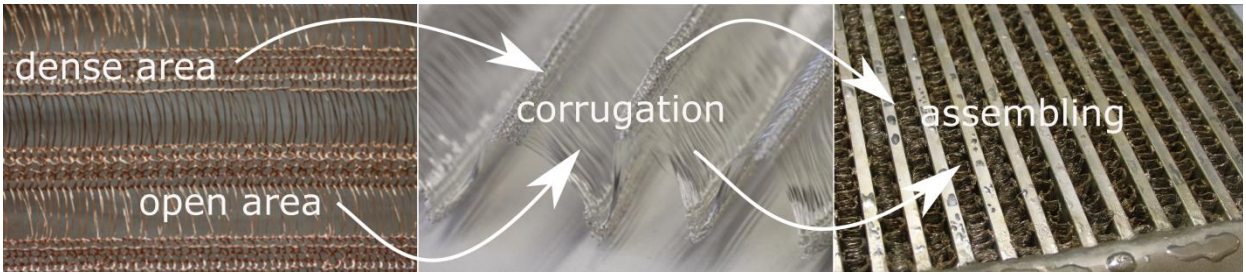

Fig. 2. Possible manufacturing process steps of wire structure heat exchanger: A knitted fabric with dense and open areas (left) is corrugated in first process step to a 3D structure (middle). In second process step dense areas are contacted to flat tubes, open areas fill space between flat tubes (right).

For flat tube heat exchangers the fabrics were corrugated, similar to standard fins (see Fig. 2, middle). More dense fabrics could be corrugated mechanically. The essential idea was to use the more open areas of the fabric as fin structure almost perpendicular to the separating walls. Thus heat conduction was not inhibited due to curvature of the wires. The more dense areas of the fabric were contacted to separating walls. A production sample for a flat tube heat exchanger is shown in Fig. 2 (right side). Therein the corrugated fabrics were

contacted with a lateral wire distance of 5.4 mm and a fin height of 10 mm to tubes of outer thickness 6.5 mm. Manufacturing feasibility could be shown in general, however two main aspects were still open. First the lateral wire distance was 2-3 times higher than comparable compact heat exchangers and corrugation was handmade. Second the contact of wire structure to the flat tubes was irregular, such that some wires were not contacted adequately. Performance measurements of heat transfer characteristics showed these limitations.

Final design of corrugated textile fabrics resembled the geometry of a market available heat exchanger from Vision4Energy [20]. The Dutch company produces a gas to gas heat exchanger used in ventilation systems. The gases flow primarily in counter-flow arrangement, separated by a dividing wall. Header and distributer are such that the both air flows are angled with respect to the wire structure block (see Fig. 3 a)). Thermodynamic and hydraulic characteristics of this heat exchanger were measured [21] at test facilities at Fraunhofer ISE [24] in order to estimate performance of heat exchangers based on corrugated textile fabrics.

Further on perpendicular flow (Fig. 3 b)) through the gas to gas heat exchanger was measured at the same test facility with one single air flow. No heat transfer took place, but pressure drop measurements could be done. Header and distributer were dismantled.

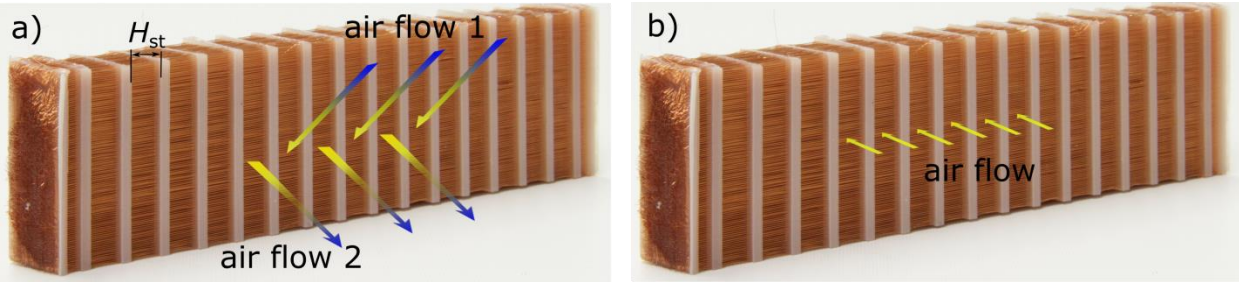

Fig. 3. Section of a gas to gas heat exchanger with continuous horizontal wires. Vertical separation wall formed by adhesive plastic. a) angled flow with two fluids (Experiment 1) in a combined counter-flow and cross-flow arrangement for determination of heat transfer characteristics; b) perpendicular flow with one fluid for determination of pressure drop characteristics (Experiment 2).

3. Performance Evaluation Criteria

The heat transfer rate $\dot{Q}_{HX}$ of a gas to liquid or gas to gas/liquid heat exchanger required for calculation of air side performance characteristics can be expressed as

$$\dot{Q}_{HX} = U_{HX}\, A_{HTS,air}\, \Delta T_m \tag{1}$$

The overall heat transfer coefficient U_{HX} is herein related to the heat transfer surface area $A_{HTS,air}$ on the air side and the true (or effective) mean temperature difference ΔT_m. The air side convection heat transfer coefficient h_{air} can be obtained from

$$\frac{1}{\eta_0 h_{air} A_{HTS,air}} = \frac{1}{U_{HX}\, A_{HTS,air}} - \frac{1}{h_w A_{HTS,w}} - \frac{\delta_{wall}}{k_{wall} A_{wall}} \tag{2}$$

The second term on the right-hand-side of Equation (2) indicates the water side thermal resistance; the third term indicates the tube wall thermal resistance. The extended surface efficiency η_0 is given in [25] for louvered and pin fins and expresses the reduction in heat transfer due to limitation in heat conduction through the heat transfer surface area enhancement.

For evaluation of measurements true mean temperature difference, heat transfer rate, water side and tube wall thermal resistance are determined (iteratively with NTU-method [25]). Since the extended surface efficiency η_0 is a function of convection heat transfer coefficient h_{air}, the value for h_{air} can be obtained from Equation (1) and (2).

Performance evaluation of heat exchangers requires comparable quantities. Different heat exchanger designs impede a comparison as different characteristic lengths, velocities and temperatures might be used. For a meaningful comparison non-dimensional and dimensional quantities are related within this study to the same

characteristic length of enhancement structure height H_{st}. The applied quantities are the Reynold number $Re_{\mathrm{H_{st}}}$, Nusselt number $\mathrm{Nu_{H_{st}}}$, friction factor $\mathrm{f_{H_{st}}}$, Prandtl number Pr_{air}, heat transfer surface area density β, structure porosity ϕ_{st} and number of transfer units on air side ntu_{air}[25]. Whereas the last one can be expressed in terms of the former ones; thus it combines specific performance information.

$$Re_{H_{st}} = \frac{v_{air,st,in}\, H_{st}}{\nu_{air}}; \qquad Nu_{H_{st}} = \frac{h_{air}\, H_{st}}{k_{air}}; \qquad f_{H_{st}} = \frac{H_{st}}{4\, L_{st}} \frac{2\, \Delta p}{\rho_{air} v_{air,st,in}^2}; \qquad Pr_{air} = \frac{\nu_{air}\, \rho_{air} c_{p,air}}{k_{air}} \tag{3}$$

$$ntu_{air} = \frac{\eta_0 h_{air} A_{HTS,air}}{\dot{m}_{air}\, c_{p,air}} = \frac{\eta_0 h_{air}}{v_{air,st,in}\, \rho_{air}\, c_{p,air}} \beta L_{st} = \frac{Nu_{H_{st}}}{Re_{H_{st}}\, Pr_{air}} \eta_0\, \beta\, L_{st} \tag{4}$$

Based on the Reynolds analogy an increase in heat transfer performance for new design heat exchangers is in general accompanied with an increase in pressure drop (or an increase in heat exchanger volume/frontal area). Thus the benefit of "heat transfer" $\eta_0 h_{\mathrm{air}} A_{\mathrm{HTS,air}}$ is paralleled by different "costs". Considering the approach of efficiency equals benefit/cost, three key figures could be defined according to Table 1.

Table 1. Key figures for extended performance evaluation; defined as benefit $\eta_0 h_{\mathrm{air}} A_{\mathrm{HTS,air}}$ per cost

Cost	Key figure	Definition	Dimension	Transformable to
Dissipated power on the air side $\Delta p_{air}\, \dot{V}_{air}$ in W, which is proportional to the power of the fans	energetic efficiency	$\frac{\eta_0 h_{air} A_{HTS,air}}{\Delta p_{air}\, \dot{V}_{air}}$	1/K	$\frac{1}{2} \frac{Nu_{H_{st}}}{f_{H_{st}}} \left(\frac{H_{st}}{Re_{H_{st}}}\right)^3 \eta_0\, \beta\, \frac{k_{air}}{\nu_{air}^3\, \rho_{air}}$
Material usage for the wire or fin structure m_{st} in kg (excluding fluid guidance, solder material and header/distributor)	mass efficiency	$\frac{\eta_0 h_{air} A_{HTS,air}}{m_{st}}$	W/(K kg)	$Nu_{H_{st}}\, \eta_0\, \beta\, \frac{k_{air}}{H_{st}} \frac{1}{\rho_{fin}(1-\phi)}$
Available volume for heat transfer enhancement V_{st} in m³ (excluding fluid guidance volume and header/distributor)	volume efficiency	$\frac{\eta_0 h_{air} A_{HTS,air}}{V_{st}}$	W/(K m³)	$Nu_{H_{st}}\, \eta_0\, \beta\, \frac{k_{air}}{H_{st}}$

All key figures are composed of the product $\mathrm{Nu_{H_{st}}} \eta_0\, \beta$, the volume specific weight $\rho_{\mathrm{fin}}(1-\phi)$ and/or the friction factor $\mathrm{f_{H_{st}}}$as well as of air/fin properties and/or $H_{st}/Re_{H_{st}}$. The latter two are kept constant for the performance evaluation in Chapter 5. The first three are considered in detail.

4. Simulation and Correlation

4.1. Simulation of Wire Structure Heat Exchanger

A cross section through a wire structure heat exchanger in direction of air fluid flow and steam fluid flow is given in Fig. 4. The cross section is based on the 2D face in Fig. 1. The cross section of the wires encompasses several circular obstacles. The air flow has to pass these obstacles before exiting the heat exchanger. The number of wires is dependent on the defined length in air flow direction, the diameter of the wires and their distance in flow direction. In this study the length of the heat exchanger (length of structure enhancement) L_{st} was defined as 40 mm. The number of wires in flow direction varied between 50 and 250, dependent on the wire distance.

Simulating flow and heat transfer around the wires in the 2D cross section can give a first estimate on the thermal hydraulic behavior of the heat exchanger. Among others, the simulation is restricted to heat exchanger geometries and operating conditions, where gradients in z-direction (perpendicular to cross section) of velocity, pressure and temperature field are negligible small (cf. [21]). In this study the wires are arranged symmetrically in x-direction, meaning that one characteristic element represents the whole geometry (see Fig. 5).

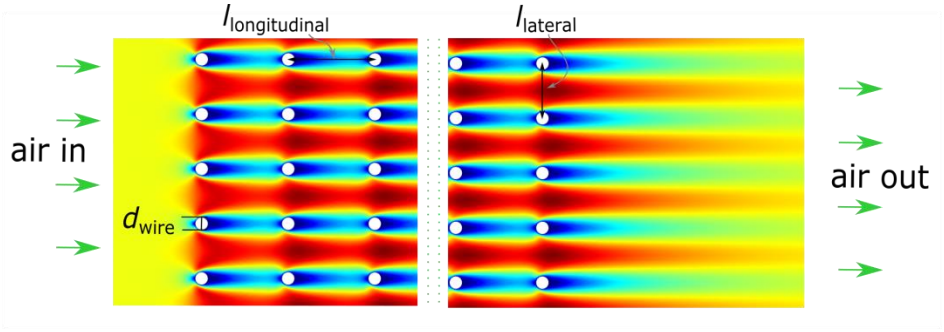

Fig. 4: Cross section through a wire structure heat exchanger according to cross section in Fig. 1. Air flow from left to right. White circles correspond to wire cross section. Higher air velocities in red, lower velocities in blue.

The characteristic element is determined by the wire diameter d_{wire}, the distances between the wires and the total length of the structure L_{st}. The distance of wires perpendicular to air flow direction is defined as lateral distance l_{lateral}, the distance of wires in flow direction as longitudinal distance $l_{\mathrm{longitudinal}}$ (see Fig. 4) . The velocity field is determined by the structure inlet velocity $v_{\mathrm{air,st,in}}$ and the structure inlet temperature $T_{\mathrm{air,in}}$.

There are no correlations for heat transfer and pressure drop vs. air velocity known from literature for the specific geometry and operating conditions used in the design concepts, thus detailed CFD simulations are necessary to obtain this information.

Laminar fluid flow and heat transfer is simulated by using the finite element method (FEM), implemented in Comsol Multiphysics® (Version 5.2). Boundary conditions for temperature, pressure and velocity are chosen according to the 2D cross section element in Fig. 5. The simplified continuity equation, Navier Stokes Equation and equation for energy conservation are describing the system on the air side.

The meshing of the domain is separated into a boundary layer fraction around the wires and a triangular mesh next to it. The 2D-simulation yields a pressure drop Δp and a convection heat transfer coefficient h_{air}.

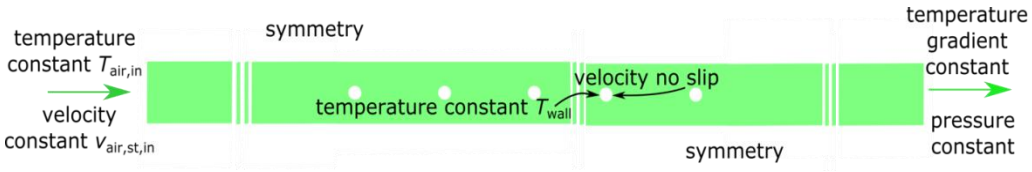

Fig. 5: Boundary conditions of simulation model. Green domain corresponds to air domain; White circles correspond to solid wire [21].

Heat transfer was assumed to take place on the wires only, not on the separating wall. Thus heat transfer rate might be underestimated with the simulation model. The geometry was varied in lateral and longitudinal wire distance, keeping $Re_{H_{st}} = 2000$ constant. The Parameters are given in Table 2.

Table 2. Parameters for 2D-Simulation of wire structure heat exchanger

Description	quantity	dimension	min	max
wire diameter	d_{wire}	mm	0.1	0.1
non-dimensional fin pitch	$a = \mathrm{l}_{\mathrm{lateral}}/d_{\mathrm{wire}}$	-	4	22
non-dimensional wire distance in air flow direction	$b = \mathrm{l}_{\mathrm{longitudinal}}/d_{\mathrm{wire}}$	-	1.5	7
height of wire structure between flat tubes	H_{st}	mm	10	10

4.2. Correlation of louvered fins

Louvered fins were used for comparison of performance. Dong [4] developed correlations for Colburn and friction factor versus Reynolds number. The geometry of louvered fins had similar dimensions as the wire structure heat exchanger design idea. The louvered fin geometry used in this study is presented in Table 3. Colburn factor (resp. Nusselt number) and friction factor were calculated according to Equation (13) and (14) in

[4]. For later comparison only one geometry with dimensional fin pitch $F_p = 2$ mmhas been selected, as smaller fin pitches are not part of Dongs study.

Table 3. Parameters of louvered fin heat exchanger (compare with [4])

Description (parameter name in [4])	Quantity in this study	dimension	value
fin thickness (δ)	d_{fin}	mm	0.1
fin height (F_h)	H_{st}	mm	10
dimensional fin pitch (F_p)	$\text{l}_{\text{lateral}}$	mm	2
non-dimensional fin pitch ($a = F_p/\delta$)	$\text{a} = \text{l}_{\text{lateral}}/d_{\text{fin}}$	-	20
louver angle (L_a)	-	°	28
louver pitch (L_p)	-	mm	1.2
louver height (L_h)	-	mm	9
fin length (L_d)	L_{st}	mm	40

5. Results

Performance evaluation was based on Nusselt number, friction factor and geometrical information. Different methods of data generation were used according to Chapter 2 and 4:

- louvered fin heat exchanger (based on correlations)
- wire Structure heat exchanger (based on angled flow; Experiment 1)
- wire Structure heat exchanger (based on perpendicular flow; Experiment 2)
- wire Structure heat exchanger (CFD-Simulation)

In Fig. 6 a) the Nusselt number is plotted versus the non-dimensional lateral fin/wire distance a. For the simulated wire structure heat exchanger the Nusselt number is decreasing with increasing lateral distance. This might be due to increasing maximum velocity through the structure for a more dense structure (lower a). The Nusselt number is increasing with increasing longitudinal distance b (distance of wires in air flow direction). A possible explanation for this might be the shadowing of wires in one row for low longitudinal distances. The Nusselt number for the experimentally determined wire structure is by a factor of 1.2 higher than for the simulated data (for appropriate a and b). This difference can be explained in part by the fact that the flow through the wire structure was not perpendicular to the structure, but angled. Thus the wires were not oriented in row but rather staggered for the inlet air. An increase in heat transfer rate and in pressure drop follows. It might be reasonably assumed that for a perpendicular air flow the Nusselt number will be smaller. Lastly the louvered fins show a low Nusselt number, a factor of 10 lower than the experimental data. However the Nusselt number of the louvered fins is in the range of wire structures with low longitudinal distance b and equal lateral distance $a = 20$.

A similar curve shape can be examined for the friction factor (see Fig. 6 b)). For the simulated wire structure friction factor is decreasing with increasing lateral distance a; sensitivity in longitudinal distance b is low for large values of a and more intense for small values of a. Friction factor for perpendicular flow (Experiment 2) was determined experimentally and shows good agreement with simulated data of equal geometry. However friction factor for angled flow (Experiment 1) could not be determined, as pressure drop at $Re_{H_{st}} = 2000$ was beyond measurement range of sensors. For $Re_{H_{st}} = 1000$ the pressure drop of angled flow was three times higher than for perpendicular flow. Friction factor for louvered fins is higher than for simulated wire structure (for equal lateral distance a). This discrepancy could be attributed to the homogenous distribution of wires on the flat tube. Small shifts of wires in lateral direction (e.g. due to manufacturing process) could increase the pressure drop significantly. This would yield a higher friction factor for the wire structures. It can be reasonably assumed that friction factor of wire structure and louvered fins for equal lateral distance is in the same dimension.

For an extended performance evaluation not only Nusselt number and friction factor are necessary, but also information on number of transfer units $\text{ntu}_{H_{st}}$on air side, heat transfer surface area density β, fin/wire structure porosity ϕ and extended surface efficiency η_0 as stated in Chapter 3. This information is given in Fig. 7. Number of transfer units is decreasing with increasing lateral wire distance for the wire structure.

Wire structure and louvered fins resemble each other for same lateral distance $a = 20$, with slightly higher values for the louvered fins. This is due to higher Nusselt number for wire structure, but lower heat transfer surface area density (see Fig. 7 b)) and lower extended surface efficiency (see Fig. 7 c)). Thus, the benefit of higher convection heat transfer rate (higher $\mathrm{Nu}_{\mathrm{H_{st}}}$) is weakened significantly for equal $a = 20$. However the benefit of mass reduction for the enhancement would still be present. As the porosity for the wire structure is between 0.97 and 0.99, the structures weight is only 20% to 60% compared to the louvered fins with a porosity of 0.95; note that the wire structure is idealized without wires for stability increase. Thus the positive effect of mass reduction will slightly decrease in real application.

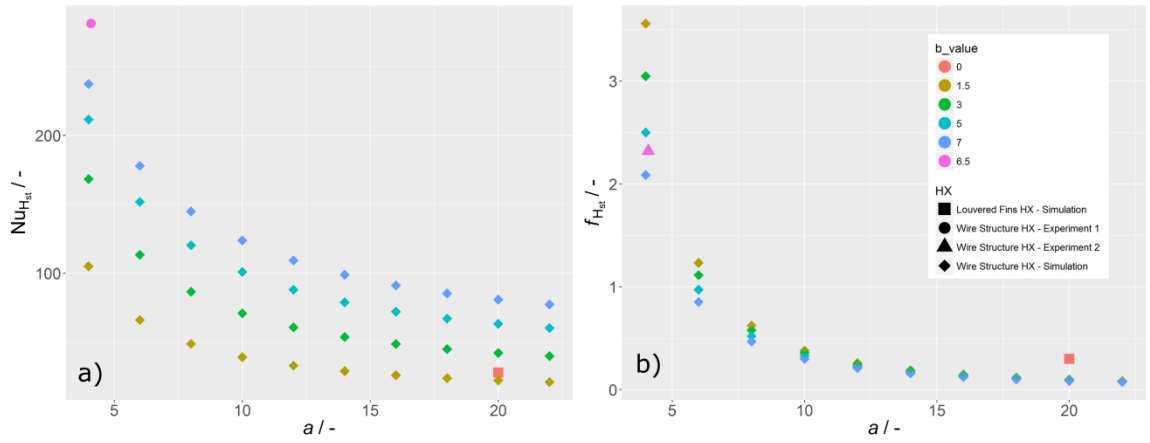

Fig. 6. Performance of different heat exchangers (HX; see shape) for different lateral fin/wire distance a (see x-axis) and different longitudinal wire distance b (see color): louvered fin heat exchanger and wire structure heat exchanger. Reynolds number $\mathrm{Re}_{H_{st}}$ equal to 2000. a) Nusselt number on air side $\mathrm{Nu}_{H_{st}}$; b) friction factor on air side $\mathrm{f}_{H_{st}}$.

For smaller lateral wire distances heat transfer surface area density is increasing for simulated wire structure. In combination with higher Nusselt numbers these geometries might be preferable. For $a = 12$ and $b = 1.5$ a similar friction factor than the reference louvered fin could be achieved with a significant higher number of transfer units (factor 1.5).With this configuration either more heat can be transferred at equal length of heat exchanger in flow direction or the length could be decreased (to 66% of louvered fin length) with the benefit of lower pressure drop and mass reduction.

Lastly values for $a = 6$ and $b = 3$ yield Nusselt numbers four times higher than louvered fins with higher surface area density. Energetic efficiency (according to Table 1) is 20% higher than for the louvered fins. More significant volume efficiency is 4.6 times higher and mass efficiency is 5.3 times higher. For the measured wire structure (with angled flow) volume and mass efficiency is even higher. However, the measured wire structure is expected to have a very low energetic efficiency at $\mathrm{Re}_{H_{st}}$, due to angled flow in header/distributor. Fig. 6 together with Fig. 7 allows a selection of appropriate geometries for individual evaporator design.

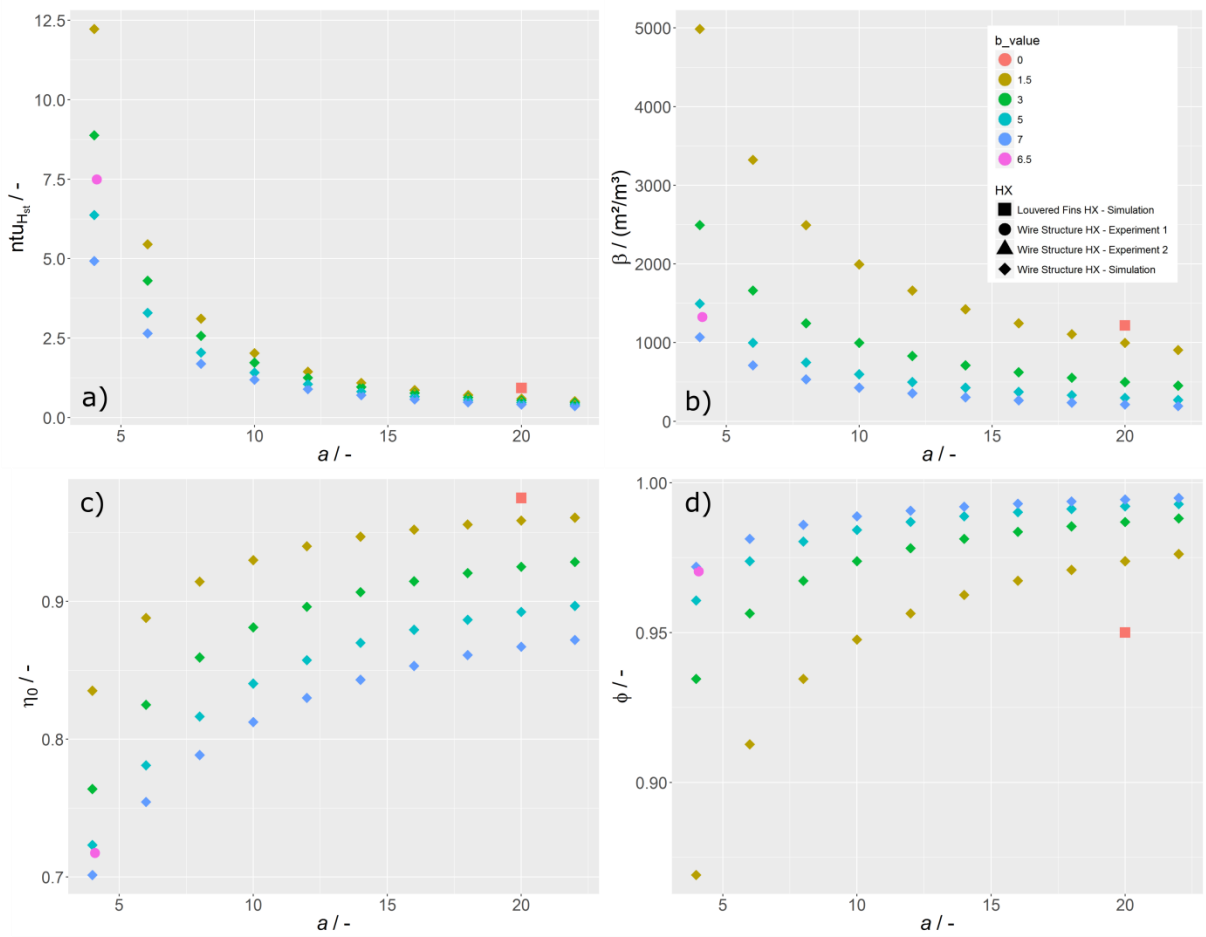

Fig. 7. Performance and design characteristics of louvered fin heat exchanger and wire structure heat exchanger (see shape) for different lateral fin/wire distance a (see x-axis) and different longitudinal wire distance b (see color). $\mathrm{Re}_{H_{st}}$ is equal to 2000. a) Number of transfer units on air side $\mathrm{ntu}_{H_{st}}$; b) heat transfer surface area density β; c) extended surface efficiency η_0; d) fin/wire structure porosity ϕ

6. Outlook to use Wire Structure Heat Exchanger for Heat Pump Evaporators

To use wire mesh heat exchangers for evaporators aspects like frosting, defrosting and condensate retention need to be investigated. The frost dynamics for conventional sheet metal fins causes leading edge frost growth and there exist no experience with wire mesh evaporators. In Fig. 8 typical frost growth dynamics is shown for staged fin configuration as one idea how to cope with inception of frost starting always in the very front of the fins.

But to deal with wires as surfaces at which frost growth will start it is important to investigate the dynamics how round tubes or wires will behave with frost on its surfaces. Literature is scarce on this topic and only for round tubes with internal evaporating flow some investigations can be found. From [26] it is known that frost layers usually build up with a relatively porous structure and frost layer thickness increases approximately parabolic with time. However, the tortuosity of the frost layer is dynamic and slowly decreases due to some inner layer frost accumulation over time. Frost growth stops almost fully when temperature difference between air humidity saturation temperature and surface temperature becomes below 1.5K [27].

Today's knowledge on the leading edge frost growth can give an idea how this could take place. Frost starts on the tip of the fins and begins growing more rapidly than on surfaces downstream due to locally higher heat transfer characteristics. This is also valid for louvered fins but means that if the multiple leading edges are not distributed equally in space – which can happen quickly in typical louvered fin topologies – the pressure drop for the air flow can become forbidden high. The wire offers equally distributed leading edges and if sized adequately it appears realistic that acceptable operation times during frost growth are possible. But also the flat tube itself

reacts like a fin leading edge. Depending on the wire surface temperature (fin efficiency) the flat tube can become the main growth area for frost with wires like pins. However the exact frost growth needs to be investigated to ensure the real behavior.

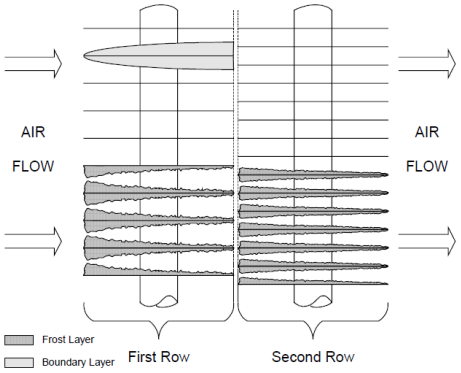

Fig. 8. Typical lateral edge frosting within a fin-and-tube heat exchanger [28]

The other two challenging parts are frost and condensate removal. Frost and ice layers will be fixed as if it stitched to the flat tube by the wires. Thus not only an initial energy transfer for melting is necessary to remove (flush) the condensate, but it is possible that segmentation and melting of ice and frost layers needs to be almost finished before it can flow down the free passages between the wire mesh. Thus any possible improvement in prolonging the operation times and heat transfer characteristics during frost needs to be compared to the additional energy demand for defrosting.

It is of decisive importance to decrease surface tensions of the wires. In experiments Nawaz [29] has shown that a compact heat exchanger with comparable louvered fin specification (than used within this work) holds back about 250 kg water per m³ unit volume of the heat exchanger whereas un-/coated aluminum metal foam with a porosity of 94,2% (10 pores per inch, pore diameter of 3,13 mm) holds back 400kg/m³ or in a state after surface treatment with the Beomite process still 100kg/m³. To reach the range of retention masses like conventional fin-and-tube heat exchangers rather small condensate masses are needed (either 80 kg/m³ in an uncoated state down to about 40 kg/m³ in case of hydrophilic coatings [30]). In case effective superhydrophilic coatings can be applied even fin pitches down to about 1.1 mm do not affect the retention significantly.

7. Summary

The potential for wire structure heat exchangers is inherent in the high heat transfer coefficient of flow around small scale obstacles. Measurements of heat transfer show convection heat transfer coefficients up to ten times higher than for louvered fins. Likewise the volume efficiency is significant higher for the wire structure heat exchanger with lateral wire distance less than $a = 10$. Additionally the volume specific weight of the wire structure is for most of the wire structure design cases less (down to 20%) compared to the louvered fin structure. Both characteristics (high volume efficiency and low volume specific weight) yield a sharp reduction of material consumption for heat transfer enhancement.

However, the high thermodynamic performance is accompanied with a low hydraulic performance for the relevant design points of small lateral wire distance. For the measured wire structure with perpendicular flow, friction factor is eight times higher than for louvered fins. Similar friction factors are reached in the simulation for analogical design. Still some geometrical design points ($a = 6, = 3$) might allow same energetic efficiency as louvered fins despite higher friction factors: The higher friction factor could be balanced with the reduction of flow length due to high volume efficiency, such that pressure drop would stay constant. The design of heat exchanger based on a parallel wire structure could allow material and volume minimization with increased volumetric thermodynamic performance without an increase in air side pressure drop.

Acknowledgements

The authors acknowledge the financial support from the German Federal Ministry of Education and Research (BMBF) for the Effimet Project [22] and the Optimat Project (FKZ 03SF0492A).

References

[1] S.-C. Costa, M. Tutar, I. Barreno, J.-A. Esnaola, H. Barrutia, D. García, M.-A. González, J.-I. Prieto, Experimental and numerical flow investigation of Stirling engine regenerator, Energy 72 (2014) 800–812.
[2] A. Kolb, E. Winter, R. Viskanta, Experimental Studies on Solar Air Collector with Metal Matrix Absorber, Solar Energy 65 (2) (1999) 91–98.
[3] A. Bejan, S.J. Kim, A. Morega, S.W. Lee, Cooling of stacks of plates shielded by porous screens, International Journal of Heat and Fluid Flow 16 (1) (1995) 16–24.
[4] J. Dong, J. Chen, Z. Chen, W. Zhang, Y. Zhou, Heat transfer and pressure drop correlations for the multi-louvered fin compact heat exchangers, Energy Conversion and Management 48 (5) (2007) 1506–1515.
[5] Y. Park, A.M. Jacobi, Air-Side Performance of Flat-Tube Louver-Fin Heat Exchangers Under Wet Conditions: Wet-Surface Multipliers for Colburn j- and f-Factors, in: IRACC, Purdue, Purdue, 2006.
[6] S. Padhmanabhan, L. Cremaschi, D.E. Fisher, J. Knight, Comparison of Frost and Defrost Performance Between Microchannel Coil and Fin-and-Tube Coil for Heat Pump Systems, in: IRACC, Purdue, Purdue, 2008.
[7] P. Zhang, Hrnjak, P. S., Air-side performance of a parallel-flow parallel-fin (PF2) heat exchanger in sequential frosting, International Journal of Refrigeration 33 (6) (2010).
[8] E. Moallem, S. Padhmanabhan, L. Cremaschi, D.E. Fisher, Experimental investigation of the surface temperature and water retention effects on the frosting performance of a compact microchannel heat exchanger for heat pump systems, International Journal of Refrigeration 35 (2012) 171–186.
[9] Y. Liu, G. Xu, X. Luo, H. Li, J. Ma, An experimental investigation on fluid flow and heat transfer characteristics of sintered woven wire mesh structures, Applied Thermal Engineering 80 (2015) 118–126.
[10] J. Xu, J. Tian, T.J. Lu, H.P. Hodson, On the thermal performance of wire-screen meshes as heat exchanger material, International journal of heat and mass transfer 50 (5-6) (2007) 1141–1154.
[11] S.B. Prasad, J.S. Saini, K.M. Singh, Investigation of heat transfer and friction characteristics of packed bed solar air heater using wire mesh as packing material, Solar Energy 83 (5) (2009) 773–783.
[12] C. Li, R.A. Wirtz (Eds.), Development of a High Performance Heat Sink Based on Screen-Fin Technology, 2003.
[13] J. Tian, T.J. Lu, H.P. Hodson, D.T. Queheillalt, H. Wadley, Cross flow heat exchange of textile cellular metal core sandwich panels, International journal of heat and mass transfer 50 (13-14) (2007) 2521–2536.
[14] Q. Li, G. Flamant, X. Yuan, P. Neveu, L. Luo, Compact heat exchangers: A review and future applications for a new generation of high temperature solar receivers, Renewable and Sustainable Energy Reviews 15 (9) (2011) 4855–4875.
[15] N. Sahiti, A. Lemouedda, D. Stojkovic, F. Durst, E. Franz, Performance comparison of pin fin in-duct flow arrays with various pin cross-sections, Applied Thermal Engineering 26 (11–12) (2006) 1176–1192.
[16] N. Sahiti, Pin fin heat transfer surfaces: Thermal and fluid dynamic performance, VDM Verlag Dr. Müller, Saarbrücken, 2008.
[17] N. Sahiti, Thermal and fluid dynamic performance of pin fin heat transfer surfaces. Dissertation, Erlangen, 2006.
[18] S. Bhunte, s. Kumbhare, Investigation of Optimum Porous Pin Fin Parameter for Forced Convective Heat Transfer through Rectangular Channel, rnal of Emerging Technology and Advanced Engineering (2014).
[19] Hiflux Ltd, Manufacturing, available at http://www.hiflux.co.uk/index.php/manufacture (accessed on July 5, 2016).
[20] Vision4Energy, Wärmetauscher, available at http://www.vision4energy.com/Waermetauscher.html.
[21] H. Fugmann, P. Di Lauro, L. Schnabel, Heat Transfer Surface Area Enlargement by Usage of Metal Textile Structures – Development, Potential and Evaluation, in: International Textile Conference, Dresden, 2016.
[22] EffiMet, EffiMet. FKZ 01LY1109C, available at http://effimet.com/index.php.
[23] L. Schnabel, F. Roell, K. Hattler, T. Studnitzky, E. Laurenz, S. Kaina, Energieeffiziente Wärmeübertragung durch 3D-Metallgewebestrukturen (EffiMet): Gemeinsamer Abschlussbericht, Techn. Informationsbibl. und Univ.-Bibl, 2015.

[24] H. Fugmann, A.J. Tahir, L. Schnabel, Woven Wire Gas-To-Liquid Heat Exchanger, in: World Congress on Mechanical, Chemical and Material Engineering, Barcelona, Avestia Publishing, International ASET Inc., Ottawa, Ontario, Canada, 2015.
[25] Shah, R. K, D.P. Sekulić, Fundamentals of heat exchanger design, Wiley, Hoboken (N.J.), 2003.
[26] S.N. Kondepudi, The effect of frost growth on finned tube heat exchangers under laminar flow. Dissertation, Texas, 1988.
[27] Seki, Fukusako, Matsuo, Uemera, Incipient phenomena of Frost Formation, Bulletin of JSME 27 (233) (1984) 2476–2482.
[28] J. Yang, A study of heat pump fin staged evaporators under frosting conditions. Dissertation, Texas, 2003.
[29] K. Nawaz, Metal Foams as novel Materials for air-cooling Heat Exchangers. Thesis, Urbana-Champaign, 2011.
[30] C.M. Korte, A.M. Jacobi, Condensate Retention and Shedding Effects on Air-Side Heat Exchanger Performance, Urbana-Champaign, 1997.